

# Self-consistent calculation of particle-hole diagrams on the Matsubara frequency: FLEX approximation

J.J. Rodríguez-Núñez

*Instituto de Física, Universidade Federal Fluminense,  
Av. Litorânea S/N, Boa Viagem,  
24210-340 Niterói RJ, Brazil.  
e-m: jjrn@if.uff.br*

S. Schafroth

*Physik-Institut der Universität Zürich,  
Winterthurerstrasse 190, CH-8057 Zürich, Switzerland.  
(July 12, 2021)*

We implement the numerical method of summing Green function diagrams on the Matsubara frequency axis for the fluctuation exchange (FLEX) approximation. Our method has previously been applied to the attractive Hubbard model for low density. Here we apply our numerical algorithm to the Hubbard model close to half filling ( $\rho = 0.40$ ), and for  $T/t = 0.03$ , in order to study the dynamics of one- and two-particle Green functions. For the values of the chosen parameters we see the formation of three branches which we associate with the a two-peak structure in the imaginary part of the self-energy. From the imaginary part of the self-energy we conclude that our system is a Fermi liquid (for the temperature investigated here), since  $\text{Im}\Sigma(\vec{k}, \omega) \approx w^2$  around the chemical potential. We have compared our fully self-consistent FLEX solutions with a lower order approximation where the internal Green functions are approximated by free Green functions. These two approaches, i.e., the fully selfconsistent and the non-selfconsistent ones give different results for the parameters considered here. However, they have similar global results for small densities.

Pacs numbers: 74.20.-Fg, 74.10.-z, 74.60.-w, 74.72.-h

## I. INTRODUCTION

High-temperature superconductors [1] a wide range of behaviour atypical [2] of the standard band-theory of metals, since at half filling they should be metals while they happen to be insulators. Then, correlations are important. This leads us to consider that the theory of strongly correlated Fermion systems plays an important role for the pairing mechanism and other properties of the cuprates [3]. The current strategy (due to Anderson) [4] to address the problem of high- $T_c$  superconductivity is to try to find a theory accounting for the normal state properties of the cuprates. This goes in analogy with the ordinary BCS theory where firstly the normal state is identified to be a Landau Fermi liquid metal and then is found an electron pairing mechanism (unknown up to now in the cuprates) which destabilizes the normal state phase towards a superconducting state. In particular, due to their pronounced two-dimensional character the one-band Hubbard Hamiltonian of the Cu-3d hole states has been taken as one of the essential models [5]. The Hubbard model is the simplest many-particle model one can write down, which cannot be reduced to a single-particle theory [6]. To study this model, the simultaneous evaluation of the frequency and momentum dependence of the one- and two-particle Green functions is crucial. Here, we adopt the opposite view of infinite dimensions [7,8] which neglects the important role of spatial correlations.

The Hubbard model has been a subject of intense numerical studies. In spite of exact diagonalization and quantum Monte Carlo studies [9–12], these methods are restricted to indeed small finite size systems. Another route which takes both dynamical as well as momentum space correlation into account is the use of diagrammatic approaches [13]. We should mention the self-consistent summation of all bubble and ladder diagrams, so called fluctuation exchange approximation, or FLEX [14–18], [19]. This approximation (FLEX) is conserving in the sense of Baym and Kadanoff [21], i.e., it is consistent with microscopic conservation laws for particle number, energy, and momentum. We recall that the FLEX approximation belongs to the class of  $\Phi$ -derivable approximations which have been discussed a long time ago by Wortis [22] in the context of perturbative series expansion of thermodynamic properties of models described by lattice Hamiltonians, mainly the Ising model. Wortis [22] gives a set of steps to construct a  $\Phi$ -derivable approximation.

In the FLEX approximation there is an interesting feature in the effective interaction: it is temperature and doping dependent through the spin susceptibility,  $\chi(\vec{q}, \omega)$ . The effective interaction depends on the properties of the

quasiparticles. One thus has a system in which, since the effective interaction both modifies the quasi-particle behavior and is itself altered by that changed quasi-particle behavior, non-linear feedback, either positive or negative, can play a significant role [23]. According to the FLEX approach, the dominant contribution to the magnetic interaction between planar quasi-particles is assumed to come from spin-fluctuation exchange, and so will be proportional to  $\chi(\vec{q}, \omega)$ . In the scheme of Pines and co-workers [23],  $\chi(\vec{q}, \omega)$  is taken from experiments, while in the present work we have a fully self-consistent close set of equations to solve.

Recently, Schmalian, Langer, Grabowski and Bennemann [24] have performed the calculation of the dynamical properties on the real axis, instead of the Matsubara frequencies. Here we perform our calculations on the Matsubara axis (1024 frequencies) obtaining the dynamical properties for all frequency range after analytically continuing the one- and two-particle Green functions with Padé approximants [25].

Our method for solving numerically the FLEX equations is based on the Fast Fourier transformation (FFT) [26] which is suitable for the evaluation of the corresponding integrals. We refer to reference [27] where this technique is documented. In order to reach high densities, while working on the imaginary time, we have started from small densities (or low chemical potential). For each value of the chemical potential we have reached self-consistency and then we move in small steps to a higher chemical potential. We have proceeded this way since the next Green function is constructed from the nearby previous one. So, we always stay close to the real solution until we reach the density we are looking for.

In Section II we describe our model Hamiltonian and the FLEX equations to be solved on the imaginary time. In Section III, we present the data for the one- and two-particle spectral functions, the self-energy and density of states. It is observed the formation of three branches in the spectral density. We analyze, following the self-consistency of our equations, the presence of these two peaks as due to the presence of two peaks in the imaginary part of the effective interaction. We have compared our solutions with a low order approximation which consists in approximating the internal Green functions by free ones. Our results show that the calculations agree globally with each other for small densities. The dynamical quantities are radically different for the density/spin investigated in this paper ( $\rho = 0.40$ ). In Section IV we discuss our result and present our conclusions.

## II. THE MODEL AND THE FLEX EQUATIONS.

The Hubbard Hamiltonian is defined as

$$H = -t \sum_{\langle ll' \rangle \sigma} c_{l\sigma}^\dagger c_{l'\sigma} + U \sum_l n_{l\uparrow} n_{l\downarrow} - \mu \sum_{l\sigma} n_{l\sigma} \quad , \quad (1)$$

where the  $c_{l\sigma}^\dagger$  ( $c_{l\sigma}$ ) are creation (annihilation) operators for electrons with spin  $\sigma$ . The number-operator is  $n_{l\sigma} \equiv c_{l\sigma}^\dagger c_{l\sigma}$ ,  $t$  is the hopping matrix element between nearest neighbours  $l$  and  $l'$ ,  $U$  is the on-site interaction and  $\mu$  is the chemical potential in the grand canonical ensemble. Here we consider a repulsive interaction,  $U > 0$ .

The one-particle Green function is expressed in terms of the self-energy,  $\Sigma(\vec{k}, i\omega_n)$ , by

$$G(\vec{k}, i\omega_n) = \frac{1}{i\omega_n - \varepsilon_{\vec{k}} - \Sigma(\vec{k}, i\omega_n)} \quad , \quad (2)$$

where  $\varepsilon_{\vec{k}} = -2t(\cos(kx) + \cos(ky)) - \mu$ . The self-energy of the Hubbard model (Eq. (1)) within the FLEX approximation is given as follows [14]

$$\Sigma(\vec{k}, i\omega_n) = \frac{T}{N} \sum_{\mathbf{q}, i\epsilon_m} V_{p-h}(\mathbf{q}, i\epsilon_m) G(\mathbf{k} - \mathbf{q}, i\omega_n - i\epsilon_m) \quad , \quad (3)$$

where the effective interaction,  $V_{p-h}(\mathbf{q}, i\epsilon_m)$ , resulting from the summation of the bubble and ladder diagrams (particle - hole channel), is given by

$$V_{p-h}(\mathbf{q}, i\epsilon_m) = \frac{U^2}{2} \chi(\mathbf{q}, i\epsilon_m) \left( \frac{3}{1 - U\chi(\mathbf{q}, i\epsilon_m)} + \frac{1}{1 + U\chi(\mathbf{q}, i\epsilon_m)} - 2 \right) \quad . \quad (4)$$

Here,

$$\chi(\mathbf{q}, i\epsilon_m) = -\frac{T}{N} \sum_{\vec{k}, i\omega_n} G(\mathbf{k} + \mathbf{q}, i\omega_n + i\epsilon_m) G(\vec{k}, i\omega_n) \quad (5)$$

is the particle-hole bubble with the renormalized Green function  $G(\vec{k}, i\omega_n)$ .  $\omega_n = (2n+1)\pi T$  and  $\epsilon_m = 2m\pi T$  are the fermionic (odd) and bosonic (even) Matsubara frequencies. Let's state that the bubble and ladder sums represent the charge and longitudinal and the transversal spin fluctuations, respectively. The effect of particle-particle fluctuations (Cooper channel) has been left out of the present study.

The previous set of equations closes with the expression for the  $\rho$  given by

$$\rho(T, \mu) = \frac{1}{2} + \frac{T}{N} \sum_{\vec{k}i\omega_n} G(\vec{k}i\omega_n) \quad . \quad (6)$$

The form of Eq. (6) is well suited for numerical calculations. It has been justified by Schafroth, Rodríguez-Núñez and Beck [27]. Eq. (6) represents a generalization of Mahan's Eq. (3.1.2) [28]. Eqs. (2-6) constitute the standard set of FLEX equations which have to be solved selfconsistently.

In order to obtain results which are independent of finite size, one should use at least some  $10^3$  Matsubara frequencies and a grid of  $30 \times 30$  lattice points. The above scheme works in principle but a closer look at the equations for  $\chi$  and  $\Sigma$  shows that the straight forward implementation of these equations does not work in practice. This is due to the 4-fold loops which would occur in the computer program. Suppose we use 2000 Matsubara frequencies and a  $30 \times 30$  grid. Then we have to carry out for every grid point and every frequency the double sum over all frequencies and all grid points. This are of the order  $(30^2 \times 2000)^2 = 3.24 \times 10^{12}$  complex operations. Even a typical super-computer would need one to several hours to make one iteration step.

Since the frequency and momentum summations are convolutions, we evaluate them using the Fast Fourier Transform (FFT). In order to do that we need to transform the FLEX equations to direct space-time. For example, Eqs. (5,3) adopt the following forms

$$\chi(\mathbf{x}, \tau) = -G(\mathbf{x}, \tau)G(\mathbf{x}, -\tau) \quad , \quad (7)$$

and

$$\Sigma(\mathbf{x}, \tau) = V_{p-h}(\mathbf{x}, \tau)G(\mathbf{x}, \tau) \quad . \quad (8)$$

In order be self-consistent, we calculate the frequency integrals on the imaginary time following a different approach to the one of Schmalian et al [24]. According to our experience, it is much better to work with Matsubara frequencies due to the fact that we have to handle neither Fermi nor Bose distribution functions. As we have previously said in the Introduction we have reached high densities by moving from a selfconsistent solution to another close by. In other words, we do not need going to real frequencies to have stability in our algorithm. In Section III we present our results, making special emphasis on the the way we have reached high densities (see Fig. 1).

### III. NUMERICAL RESULTS AND INTERPRETATION

In Fig. 1 we present the density/spin,  $\rho$ , as function of chemical potential,  $\mu$ , for  $U/t = 4.0$  and a temperature of  $T/t = 0.03$ . (This temperature is slightly above the temperature used in Ref. [24] of Schmalian et al. We have chosen this temperature since we can recover the asymptotic behavior, i.e.,  $\pi * 512 * T = 45t \approx 11.1U$ . For  $T/t < 0.03$  we need to increase the number of Matsubara frequencies (we would need to go to RAM memories of 100 Mb or higher) in order to reach the asymptotic behavior. This asymptotic behavior is needed in order to compute the Fast Fourier transforms. In this figure we also show the the equivalent results for a low order approximation which consists in replacing in Eqs. (3-5) the full one-particle Green function,  $G(\vec{k}, i\omega_n)$ , by the one-particle free Green function,  $G_o(\vec{k}, i\omega_n) = 1/(i\omega_n - \epsilon_{\vec{k}})$ . This approximation was proposed by Serene and Hess [29]. We observe that the two curves almost coincide for low densities. For high densities, this is not the case, as we will see shortly. At this point we would like to emphasize that the way we have reached high densities settles the apparent drawbacks of the calculations of the  $T$ -matrix approach which is a lower order approximation to FLEX. There is recent calculation by Kagan et al [30] where they have performed analytical calculations for the negative Hubbard model in the frame of the  $T$ -Matrix approximation.

In Fig. 2 we present the spectral density,  $A(\vec{k}, \omega)$ , as function of frequency,  $\omega$  for different momenta along the diagonal of the Brillouin zone  $(k, k) = \pi/16(n, n)$ , with  $n$  an integer. We have the parameters  $U/t = 4.0$ ,  $T/t = 0.03$ ,  $\rho = 0.40$ . We are working with a system of  $32 \times 32 \times 1024$ . The function  $A(\vec{k}, \omega)$  is obtained from the one-particle Green function by means of the analytical continuation,

$$A(\vec{k}, \omega) \equiv -\frac{1}{\pi} \lim_{\delta \rightarrow +0} \text{Im}[G(\vec{k}, \omega + i\delta)] \quad . \quad (9)$$

In Eq. (9), we have chosen  $\delta/t = 0.01$ . After selfconsistency, the chemical potential turns out to be  $\mu = -0.95$ . We should like to point out that the chemical potential is independent of  $\delta$ . This value is used at the end of the calculations to perform the analytical continuation as done by Vidberg and Serene [25]. See also Ref. [24] for more details. From Fig. 2 we see that the spectral functions have a well defined peak for small momenta and a satellite for positive frequency. For large momenta, we observe a kind of *incoherent peak* for positive frequencies and a satellite for negative frequencies. This *incoherent* peak could be decomposed into two peaks, one for small positive frequencies and another one for large positive frequencies. These results are different with respect to the negative Hubbard model at small density (T-Matrix Approximation), since in the T-Matrix approximation we find two peaks in the one-particle spectral function, while here we are resolving three peaks, instead. The relevance of the spectral functions in the Hubbard model both above and below the critical temperature,  $T_c$  of the superconducting state has been treated by Dahm and Tewordt [19] (See their Figs. 17). They have compared their spectra with photoemission data of  $La_{2-x}Sr_xCuO_4$ .

For comparison, in Fig. 3, we present the spectral densities for the low order approximation. We observe that the peak structure is more pronounced than in the interacting case. This effect is also seen in the self-energy which we show next.

In Fig. 4 we display the imaginary part of the self-energy,  $-Im[\Sigma(n, n, \omega)]$ , along the diagonal of the Brillouin zone. The parameters are the same as in Fig. 2. We observe that energy dependence of  $-Im[\Sigma(n, n, \omega)]$ , close to the chemical potential (the chemical potential is located at  $\omega = 0$ ), has a gap-like structure.  $-Im[\Sigma(n, n, \omega)]$  has a well defined gap structure close to the chemical potential ( $\omega \approx 0$ ). We also see two almost symmetric peaks for every moment ( $k, k$ ). This presents a difference with respect to the attractive Hubbard model at small densities. For the attractive Hubbard model at small densities, there was a single peak in frequency for all values of ( $k, k$ ). This single peak structure in  $-Im[\Sigma(n, n, \omega)]$  was fitted by a two-pole Ansatz for the one-particle Green function. From Fig. 4 we conclude that, for the studied temperature, we have a Fermi liquid system, since  $Im\Sigma(\vec{k}, \omega) \approx \omega^2$  for  $\omega$  close to the chemical potential. We agree with Wermbtx [20] even when his calculation is mean-field like. See the discussion of Fig. 5.

In Fig. 5 (a) we present the same quantity,  $-Im[\Sigma(n, n, \omega)]$  vs  $\omega$ , for the low order approximation. We immediately see a well defined gap for high momenta. In consequence, the effect of fluctuations is to reduce the exaggerated gap of the non-selfconsistent solution. Replacing our internal lines by free Green functions is equivalent to stay close to mean-field treatments, as it has been done by Kampf and Schrieffer [31]. These authors find well defined gaps in the spectral density which are most likely due to their mean field treatment. The approach mentioned in Ref. [31] has been critically studied by Monthoux [32]. In Fig. 5 (b) we show  $-Im[\Sigma(n, 0, \omega)]$  vs  $\omega$ . Here the gap is present for all the momenta.

As it has been said in the Introduction the effective potential is strongly momentum and frequency dependent. We show in Figs. 6 and 7 the imaginary and real parts of the effective potential, respectively, for the same set of parameters as given in Fig. 2 along the diagonal of the Brillouin zone. We observe that  $Im[V_{p-h}(m, m, \omega)]$  ( $Re[V_{p-h}(m, m, \omega)]$ ) is basically odd (even) in frequency around the chemical potential. This symmetry around zero is due to the fact that the Hartree shift (HS) has been subtracted from the effective interaction. The real part of the effective interaction, i.e.,  $Re[V_{p-h}(m, 0, \omega)]$  vs  $\omega$  compares qualitatively well with Fig. 19(a) of Ref. [19]. The authors of Ref. [19] have plotted the irreducible spin susceptibility,  $\chi(\vec{k}, \omega)$  vs  $\omega$  for some values of  $\vec{k}$ .

Now, we are in a position to explain the double peak structure in the imaginary part of the self-energy. Going to real frequencies, Eq. (3) can be rewritten as

$$\begin{aligned} \Sigma(\vec{k}, z) = & \frac{1}{N} \sum_{\vec{q}} \left[ \int_{-\infty}^{+\infty} d\omega V_{p-h}(\mathbf{q}, z - \omega) A(\vec{k} - \vec{q}, \omega) n_F(\omega) \right. \\ & \left. - \int_{-\infty}^{+\infty} \frac{d\omega}{\pi} Im[V_{p-h}(\vec{q}, \omega)] n_B(\omega) G(\vec{q} - \vec{k}, -\omega + z) \right] \quad , \end{aligned} \quad (10)$$

where  $n_F(\omega)$  and  $n_B(\omega)$  are the Fermi and Bose distribution functions, respectively.

As the peaks of  $Im[V_{p-h}(\vec{q}, \omega)]$  are symmetric in energies, then both terms of Eq. (10) contribute. As  $Im[V_{p-h}(\vec{q}, \omega)]$  is antisymmetrical for frequencies close to  $\mu$  where  $A(\vec{k}, \omega)$  has a peak, then we have two contributions to  $Im[\Sigma(\vec{k}, \omega)]$ . Indeed, the numerical results for any ( $k, k$ ) of the self-energy mirror the behavior of  $V_{p-h}(\vec{q}, \omega)$ . Thus, the two-particle spectrum is introduced into the one-particle quantities like  $G(\vec{k}, \omega)$  and  $A(\vec{k}, \omega)$ .

## IV. CONCLUSIONS.

The FLEX approximation, a Baym-Kadanoff generalization of Hartree-Fock theory, has been implemented to study the frequency and momentum dependence of the one- and two-particle correlation functions. We have found the existence of three peaks in the one-particle spectral density, for the set of parameters investigated here. The presence of this structure in the spectral functions is a clear manifestation that correlations are indeed important. For smaller density/spin, for example  $\rho = 0.1$  (Fig. 8), we find that the spectral functions are almost single peaks, or free-like quasi-particles. We have compared our self-consistent calculation with a low order approximation which consists in replacing the internal one-particle Green functions by free ones. The effects of the latter approximation are evident: the spectral functions are almost delta functions and the self-energy shows a wide gap around the chemical potential, which signals that this approximation is mean-field-like. We add that besides the good features present in the FLEX approximation [33], we have shed some light on another aspect of it, i.e., the dependence of the one-particle properties on the two-particle Green functions due to the self-consistency of the FLEX equations. We mention the work of Nakamura, Moriya and Ueda [34] and references therein where they point out the role of both the low and high frequency behavior of the spin fluctuations in the superconducting phase. For densities around half-filling correlations start to build in giving rise to three peaks in the energy spectrum. We argue that this analysis can be described in a generalized scheme of three-pole Ansatz for the spectral function [35]. Work along these line is in progress [36] in order to really resolve the three peaks in the one-particle spectral function. We should add that three peaks in the  $A(\vec{k}, \omega)$  is equivalent to two peaks in the imaginary part of the self-energy. In this work, we have also discussed the differences of FLEX with respect to the  $T$ -Matrix approximation.

## V. ACKNOWLEDGMENTS.

We would like to thank Brazilian Agency CNPq (Project No. 300705/95-96), CONDES-LUZ and CONICIT (Project No. F-139). Very useful discussions with Profs. M.S. Figueira, E.V. Anda, M.A. Continentino, A.M. Rodero and H. Beck are fully acknowledged. We appreciate Prof. G. Martínez for calling our attention to references [18], [24]. We thank Prof. María Dolores García González for reading the manuscript.

- 
- [1] J.G. Bednorz and K.A. Müller, *Z. Phys. B* **64**, 189 (1986).
  - [2] J.R. Schrieffer, *Physica Scripta* **T42**, 5 (1992).
  - [3] Elbio Dagotto, *Rev. Mod. Phys.* **66**, 763 (1994).
  - [4] P.W. Anderson, *Science* **235**, 1196 (1987); see also, José González, Miguel A. Martín Delgado, Germán Sierra and Angeles José Vozmediano, *Quantum Electron Liquids and High- $T_c$  Superconductivity*, Springer (1995), where the authors give a nice introduction to the Hubbard model and its connection with the cuprates.
  - [5] There is some recent calculations in strongly correlated electron systems where an additional interaction,  $W$ , is introduced. See for example, D.J. Scalapino, " Does the Hubbard model have the right stuff?", in *International School of Physics Enrico Fermi*, Course CXXI, edited by R.A. Broglia and J.R. Schrieffer. North-Holland (1994); F.F. Assaad, M. Imada and Douglas Scalapino, Technical Report of ISSP. Series Q, No. 3187.
  - [6] Assa Auerbach, *Interacting Electrons and Quantum Magnetism*. Springer-Verlag (1994). Chapter 3.
  - [7] Antoine Georges, Gabriel Kotliar, Werner Krauth and Marcelo J. Rozenberg, *Rev. Mod. Phys.* **68**, 13 (1996).
  - [8] D. Vollhardt, in *Correlated Electron Systems*, edited by V.J. Emery (World Scientific, Singapore). 1993.
  - [9] E. Dagotto, A. Nazarenko, and M. Bonisengi, *Phys. Rev. Lett.* **73**, 728 (1994).
  - [10] N. Bulut, D.J. Scalapino and S.R. White, *Phys. Rev. Lett.* **72**, 705 (1994).
  - [11] R. Preuss, W. Hanke and W. von der Linden, *Phys. Rev. Lett.* **75**, 1344 (1995).
  - [12] Thomas Husslein, Werner Fettes and Ingo Morgenstern, *Int. J. Modern Phys. C* **8**, 397 (1997). They have calculated the ground state of the Hubbard model obtained by Quantum-Monte Carlo simulations and they have compared from exact results from exact and stochastic diagonalizations. Their system size is  $4 \times 4$ .
  - [13] Alexei M. Tsvelik, *Quantum Field Theory in Condensed Matter Physics*. Cambridge (1996). Chapter 5.
  - [14] N.E. Bickers and D.J. Scalapino, *Ann. Phys. (N.Y.)* **193**, 206 (1989).
  - [15] N.E. Bickers, D. J. Scalapino and S.R. White, *Phys. Rev. Lett.* **62**, 961 (1989).
  - [16] N.E. Bickers and S.R. White, *Phys. Rev. B* **43**, 8044 (1991).
  - [17] W. Serene and D.W. Hess, *Phys. Rev. B* **44**, 3391 (1991).

- [18] C.-H. Pao and N.E. Bickers, Phys. Rev. B **49**, 1586 (1994).
- [19] T. Dahm and L. Tewordt, Phys. Rev. B **52**, 1297 (1995); see also, T. Dahm and L. Tewordt, Phys. Rev. Lett. **74**, 793 (1995). These calculations are done self-consistently on the real frequency axis.
- [20] S.W. Wernbtext, Phys. Rev. B **55**, R10149 (1997).
- [21] Leo P. Kadanoff and G. Baym, *Quantum Statistical Mechanics*. Advanced Book Classics, Addison-Wesley Publishing Company (1989); G. Baym and Leo P. Kadanoff, *Phys. Rev.* **124**, 287 (1961); G. Baym, *Phys. Rev.* **127**, 1391 (1962).
- [22] Michael Wortis, in *Phase Transitions and Critical Phenomena*. Vol. 3, pp. 113. Edited by C. Domb and M.S. Green. Academic Press (1974).
- [23] D. Pines, Z. für Physik B **103**, 129 (1997).
- [24] J. Schmalian, M. Langer, S. Grabowski and K.H. Bennemann, Computer Phys. Commun. **93**, 141 (1996).
- [25] H.J. Vidberg and J.W. Serene, J. Low Temp. Phys. **29**, 179 (1979); also, cond-mat/9612426.
- [26] Paul L. Devries, *A First Course in Computational Physics*. John Wiley and Sons, Inc. (1994). Chapter 6. See also Ref. [27].
- [27] S. Schafroth, J.J. Rodríguez-Núñez and H. Beck, J. Phys.: Condens. Matter, **9**, L111 (1997).
- [28] Gerald D. Mahan, *Many-Particle Physics*, Second Edition. Plenum (1990). Mahan's Eq. (3.1.2) is probably incorrect. One way to calculate  $\rho$  is by means of  $n_F(\varepsilon_{\vec{p}}) = 1/2 + T \sum_{-\infty}^{+\infty} [1/(i\omega_n - \varepsilon_{\vec{p}}) - 1/i\omega_n]$ . The term inside braces, for large  $n$ —scales likes  $1/n^2$  even where the first term is replaced by the full  $G(\vec{p}, i\omega_n)$ . We leave this task for a future calculation.
- [29] W. Serene and D.W. Hess, Phys. Rev. B **43**, 8044 (1991).
- [30] Maxim Yu. Kagan, Raymond Frésard, Massimiliano Capezzali and Hans Beck, cond-mat/9704136.
- [31] A. Kampf and J.R. Schrieffer, Phys. Rev. B **42**, 7967 (1990); see also, J.R. Schrieffer, " Weak-Coupling Approach to Strongly Correlated Fermions", in *International School of Physics Enrico Fermi*, Course CXXI, edited by R.A. Broglia and J.R. Schrieffer. North-Holland (1994).
- [32] P. Monthoux. Pre-print (1996).
- [33] T. Dahm, Solid State Commun. **101**, 487 (1997); see also T. Dahm, D. Manske and L. Tewordt, Z. Phys. B **102**, 323 (1997) and S. Grawowski, J. Schmalian, M. Langer and K.H. Bennemann, Phys. Rev. B **55**, 2784 (1997). These two papers apply the FLEX approximation to study the bilayer HTc superconductors.
- [34] T. Moriya and K. Ueda, J. Phys. Soc. Japan **63**, 1871 (1994); S. Nakamura, T. Moriya and K. Ueda, ibidem **65**, 4026 (1996). The theory of these authors is a second order approximation to FLEX. The FLEX approximation has been used by S. Grabowski, M. Langer, J. Schmalian and K.H. Bennemann to study the superconducting properties of the cuprates with doping.
- [35] W. Nolting, Z. Physik **225**, 25 (1972).
- [36] J.J. Rodríguez-Núñez and M. Argollo de Menezes cond-mat/1997; see also, J.J. Rodríguez-Núñez, E. Anda and M.S. Figueira (Unpublished).

## Figures.

FIG. 1. The density/spin,  $\rho$  as function of chemical potential,  $\mu$  for the full self-consistent FLEXC equations as given in Eqs. (2,6). We also show the results for a low order approximation where we substitute the internal one-particle Green functions by free Green functions. The parameters used here are  $U/t = 4.0$ ,  $T/t = 0.03$ .

FIG. 2. The diagonal one-particle spectral function,  $A(n(\pi, \pi), \omega)$  vs  $\omega$  for different momenta along the diagonal of the Brillouin zone ( $\vec{k} = (n, n)\pi/16$ ) for  $U/t = 4.0$ ,  $T/t = 0.03$ . We have used an external damping of  $\delta/t = 0.01$ ,  $32 \times 32$  points in the Brillouin zone and 1024 Matsubara frequencies. After self-consistent calculation of the coupled non-linear equations, we get  $\mu/t = -0.9558$ . We have runned our source code in single precision requiring 43 MB of RAM memory. Each iteration takes 3.2 minutes of CPU time in a Pentium 166.

FIG. 3. The diagonal one-particle spectral function,  $A(n(\pi, \pi), \omega)$  vs  $\omega$  for different momenta along the diagonal of the Brillouin zone ( $\vec{k} = (n, n)\pi/16$ ) for the low order approach. Same parameters as in Fig. 2. Here we have taken  $\delta/t = 0.0001$ .

FIG. 4.  $-Im[\Sigma(n(\pi/16, \pi/16), \omega)]$  vs  $\omega$  for different momenta along the diagonal of the Brillouin zone ( $\vec{k} = (n, n)\pi/16$ ). Same parameters as in Fig. 2.

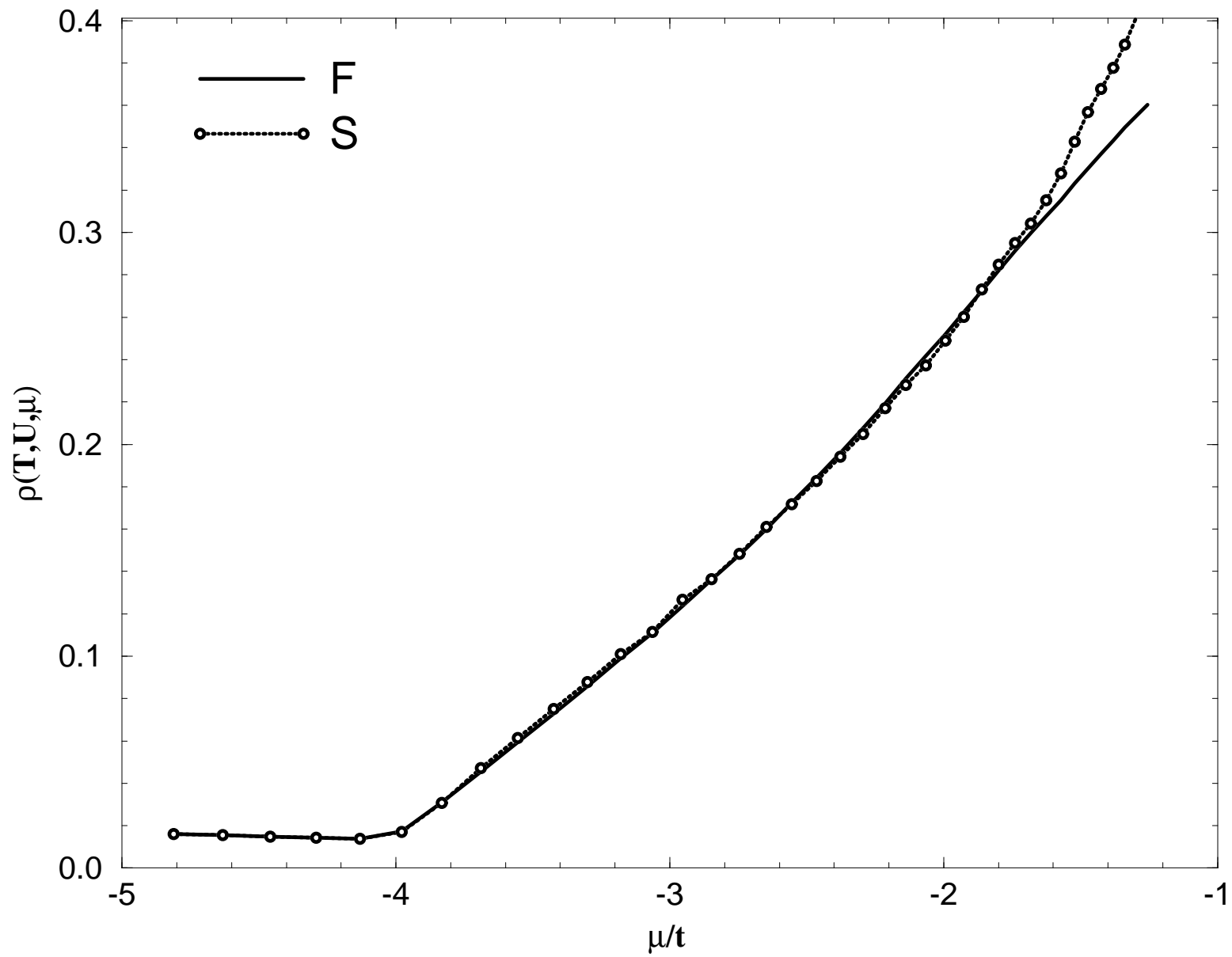
FIG. 5. (a)  $-Im[\Sigma(n(\pi/16, \pi/16), \omega)]$  vs  $\omega$  for different momenta along the diagonal of the Brillouin zone ( $\vec{k} = (n, n)\pi/16$ ) for the low order approximation. Same parameters as in Fig. 2.  $\delta/t = 0.0001$ . (b)  $-Im[\Sigma(n(\pi/16, o), \omega)]$  with the same parameters.

FIG. 6.  $Im[V_{p-h}(m(\pi/16, \pi/16), \omega)]$  vs  $\omega$  for different momenta along the diagonal of the Brillouin zone ( $\vec{q} = (m, m)\pi/16$ ). Same parameters as in Fig. 2. To simplify a little bit the notation, we have identified the effective potential,  $V_{p-h}(m(\pi/16, \pi/16), \omega)$  by  $T(m(\pi/16, \pi/16), \omega)$ . The same is done in the next figure.

FIG. 7.  $Re[V_{p-h}(m(\pi/16, \pi/16), \omega)]$  vs  $\omega$  for different momenta along the diagonal of the Brillouin zone ( $\vec{q} = (m, m)\pi/16$ ). Same parameters as in Fig. 2.

FIG. 8. The diagonal one-particle spectral function,  $A(n(\pi, \pi), \omega)$  vs  $\omega$  for different momenta along the diagonal of the Brillouin zone ( $\vec{k} = (n, n)\pi/16$ ). Here the density/spin is 0.1 and  $\mu = -3.17t$ .

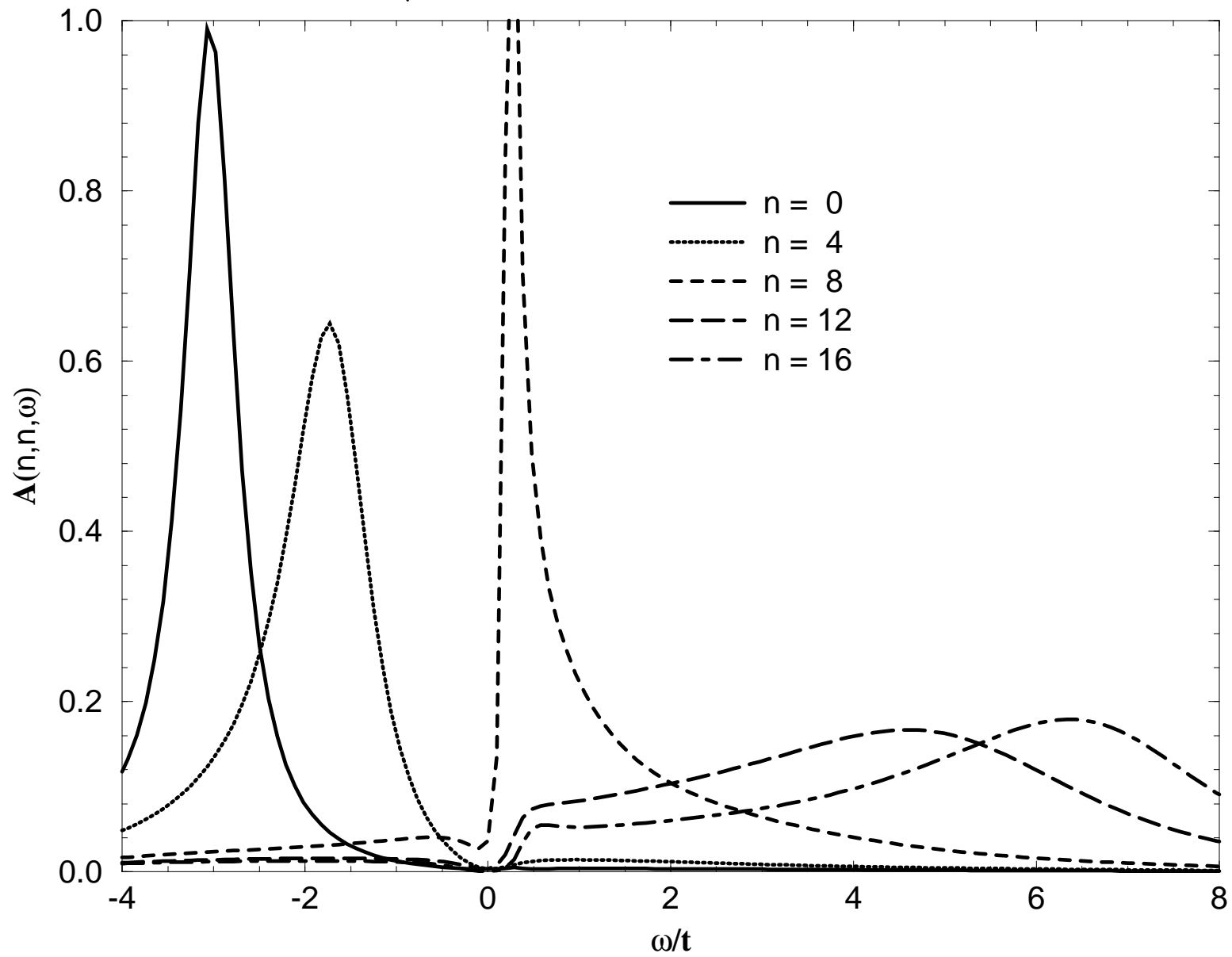
**$T/t = 0.03$   $U/t = 4.0$**





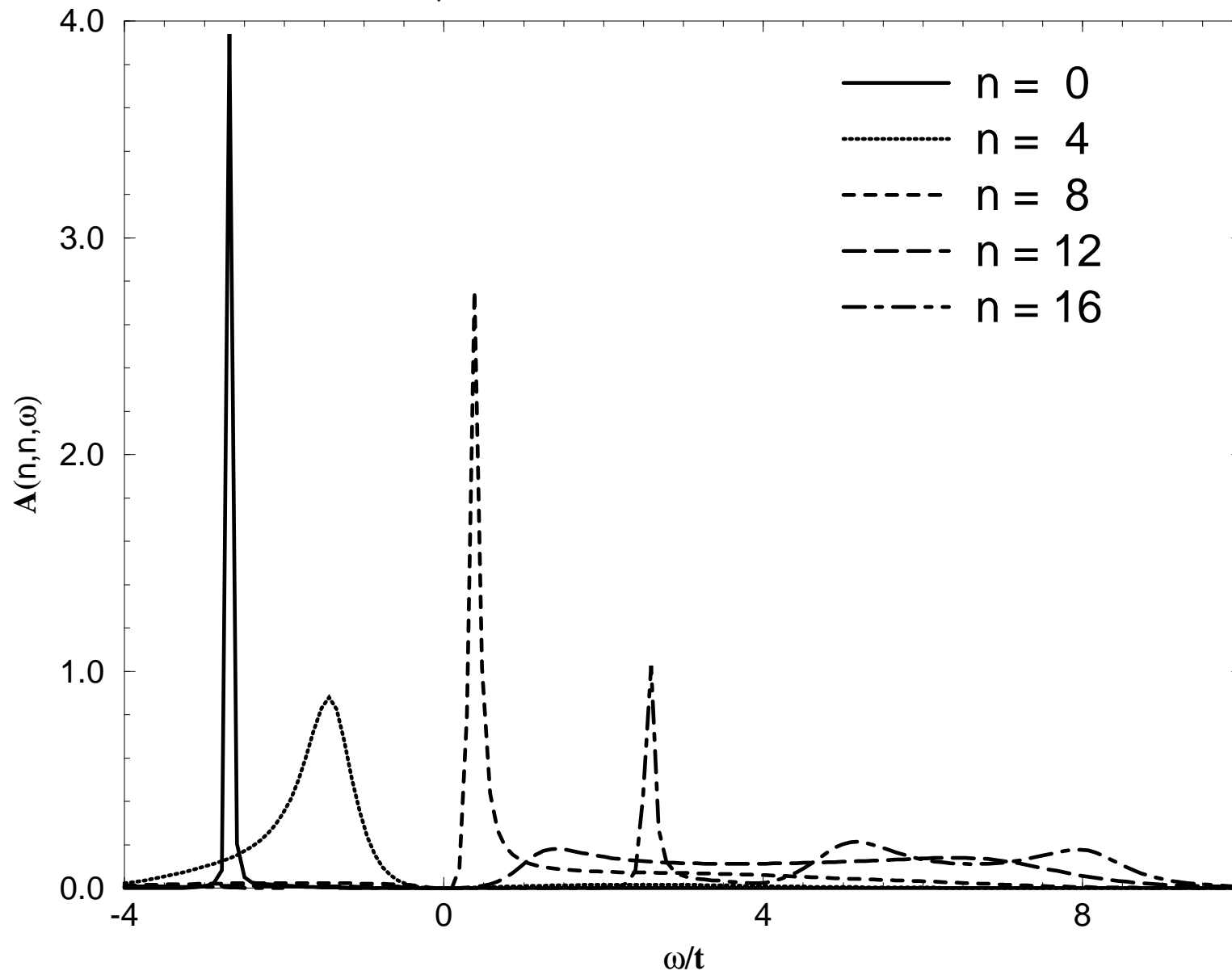
**$U/t = 4.0$   $T/t = 0.03$   $\rho = 0.40$**

**$\mu/t = -0.9558$   $\delta/t = 0.01$   $32*32*1024$**



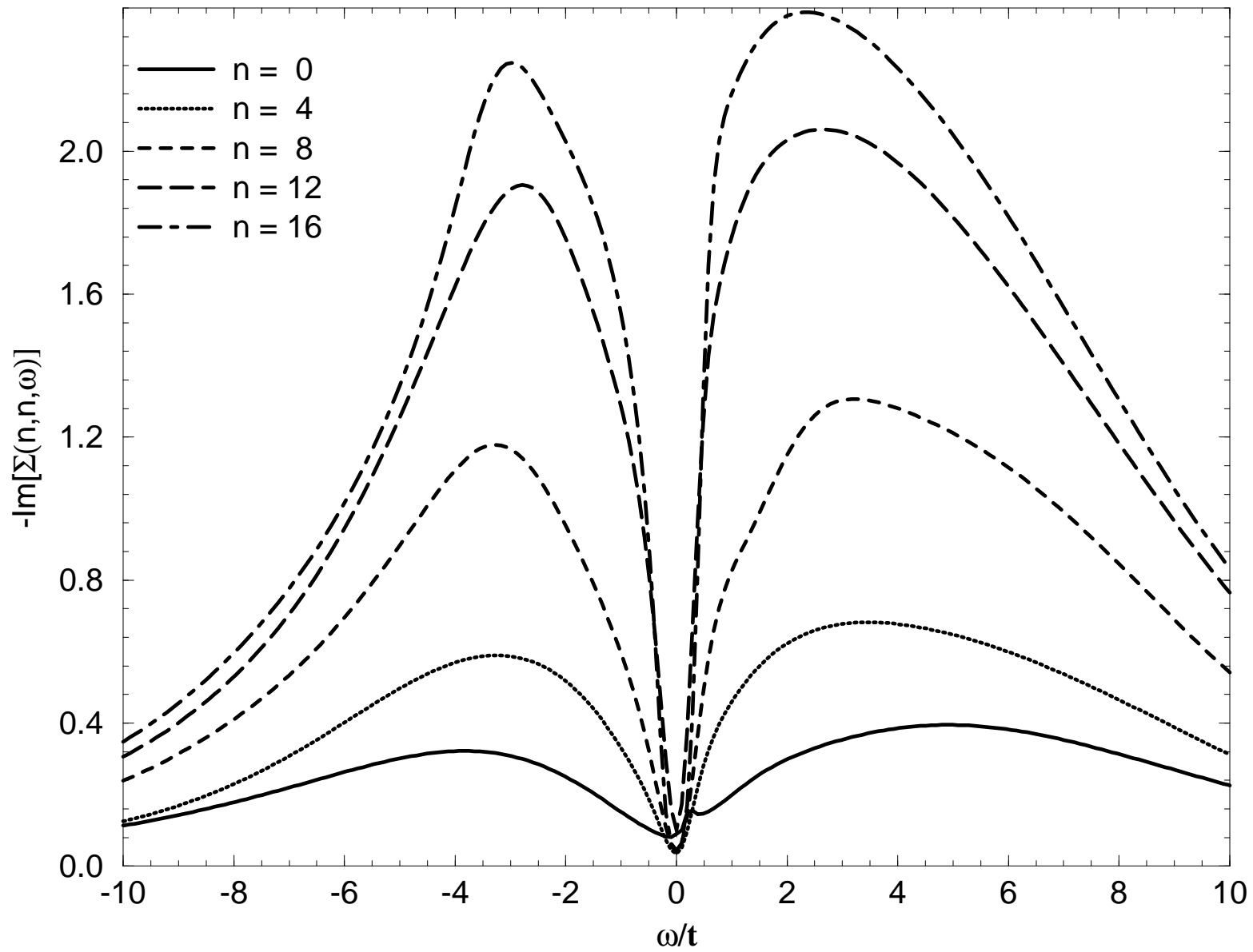
**$U/t = 4.0$   $T/t = 0.03$   $\rho = 0.40$**

$\mu/t = -1.303$   $\delta/t = 0.0001$  Serene



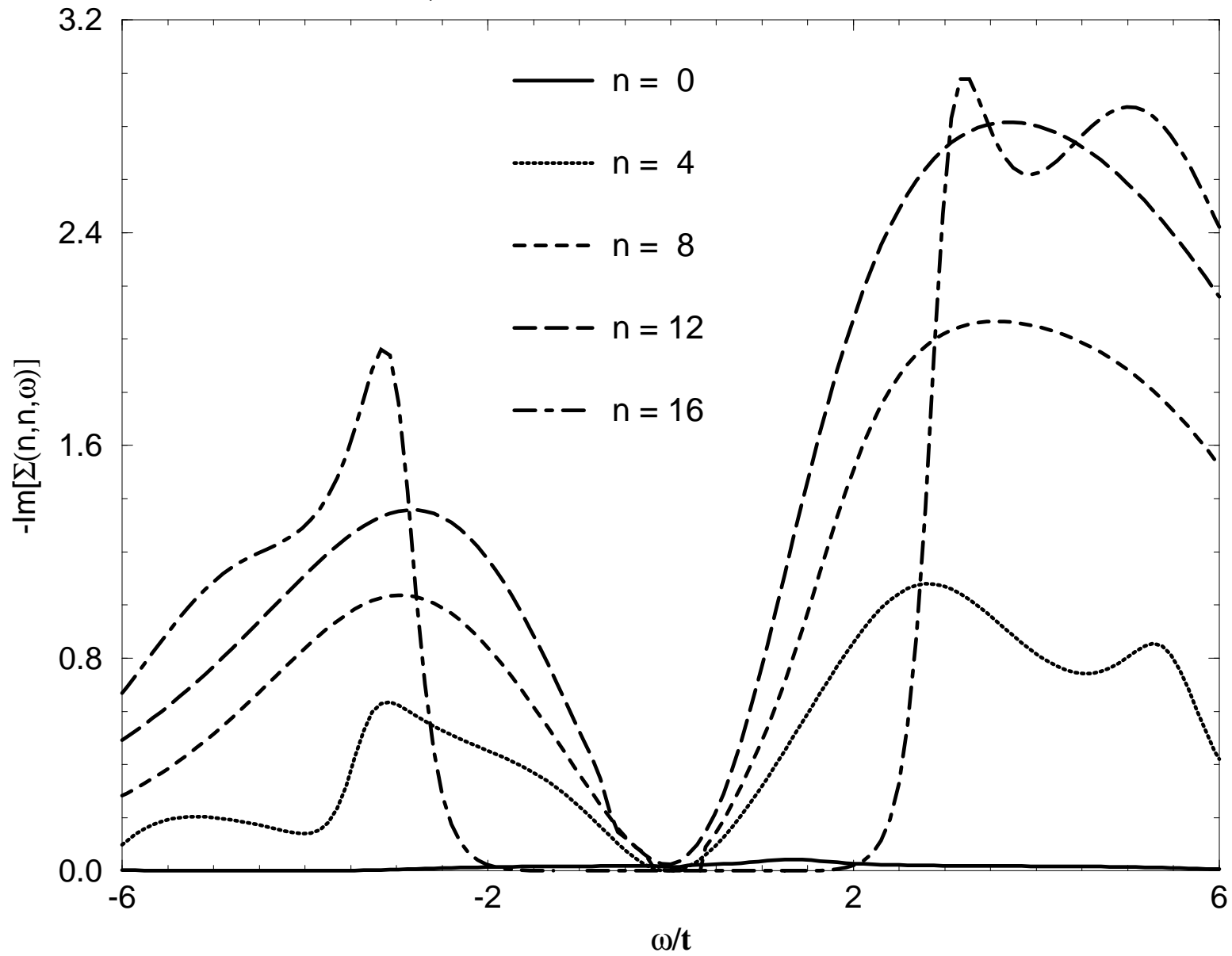
**$U/t = 4.0$   $T/t = 0.03$   $\rho = 0.40$**

**$\mu/t = -0.9558$   $\delta/t = 0.01$   $32*32*1024$**



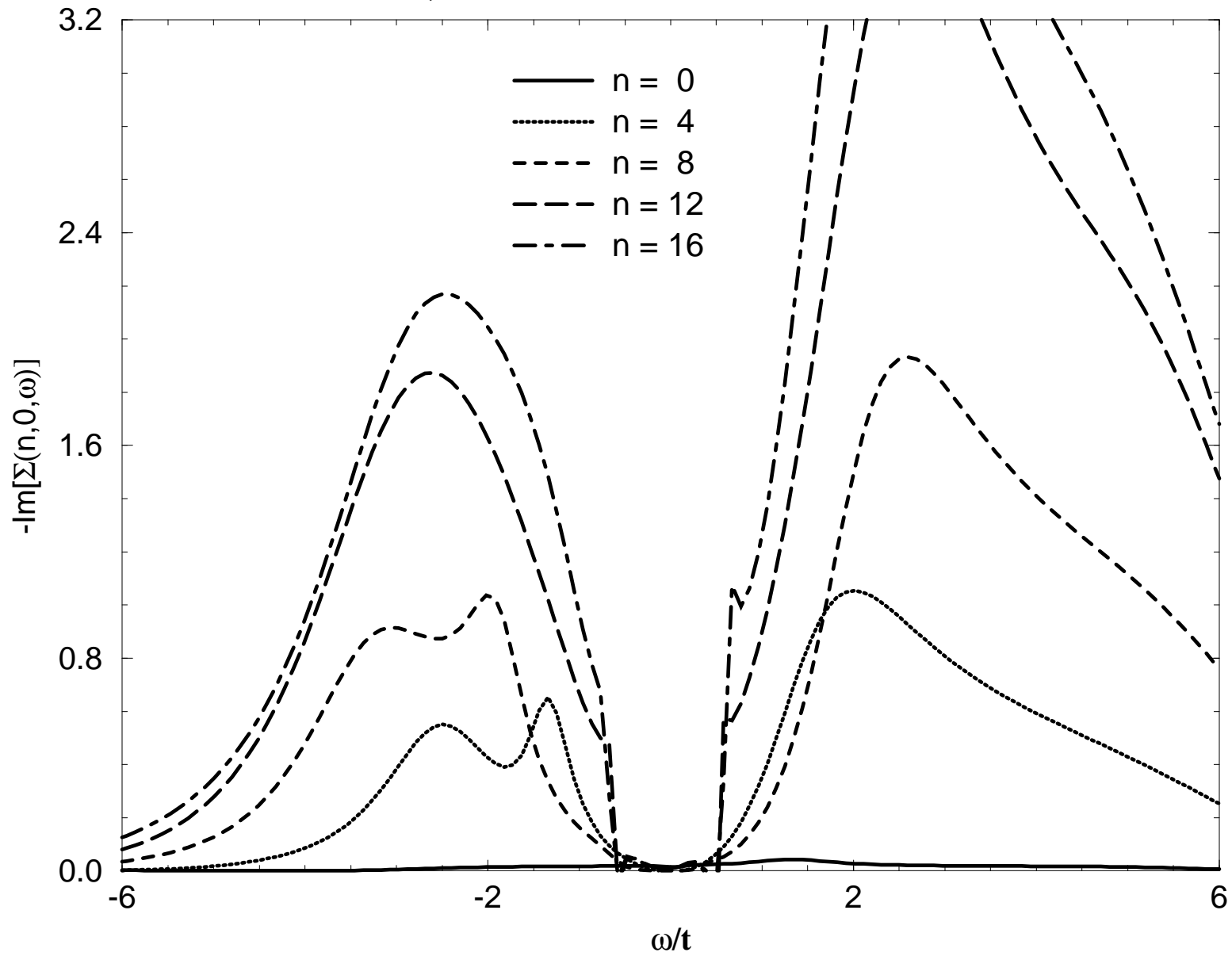
**$U/t = 4.0$   $T/t = 0.03$   $\rho = 0.40$**

$\mu/t = -1.303$   $\delta/t = 0.0001$  Serene



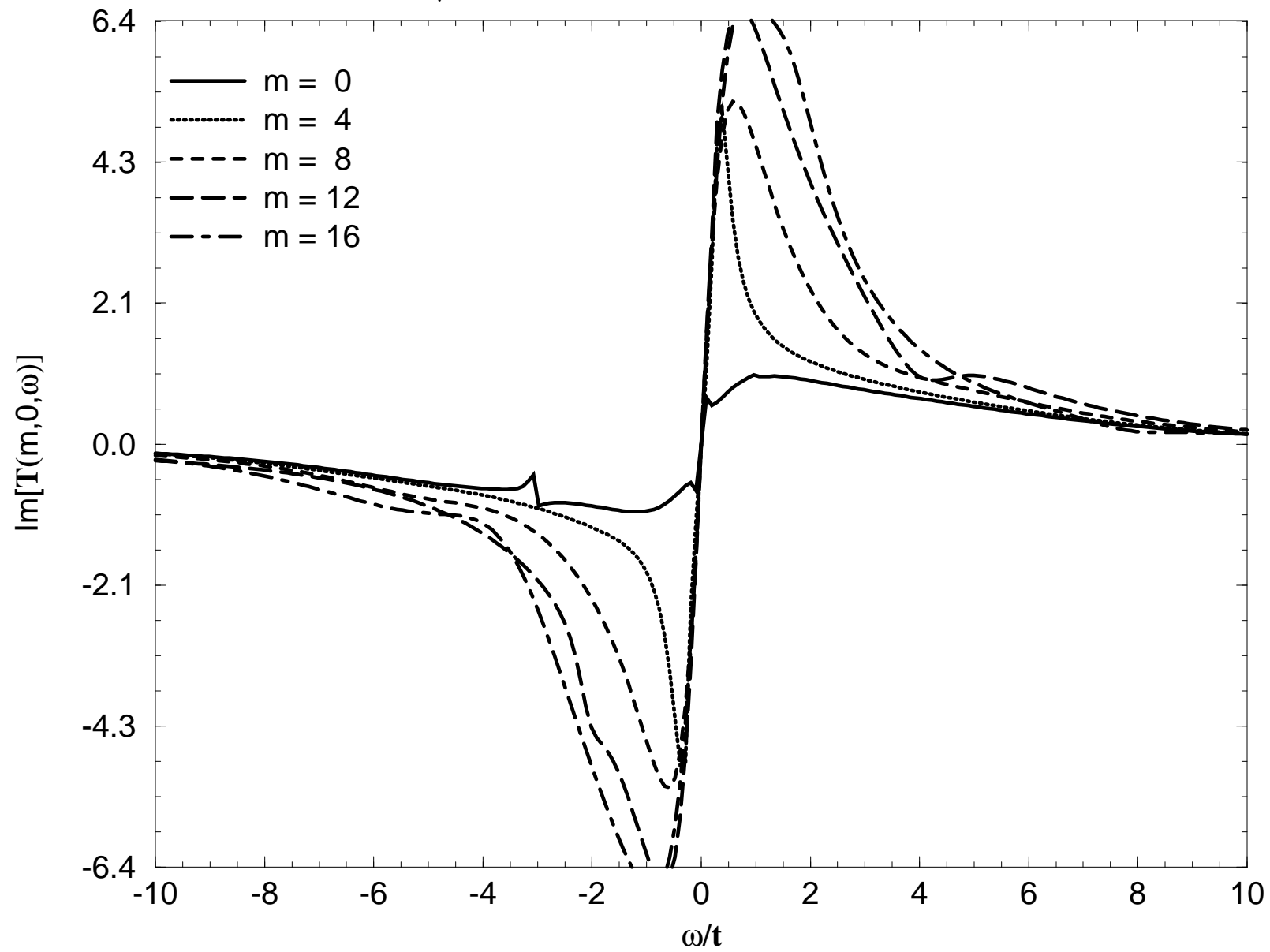
**$U/t = 4.0$   $T/t = 0.03$   $\rho = 0.40$**

$\mu/t = -1.303$   $\delta/t = 0.0001$  Serene



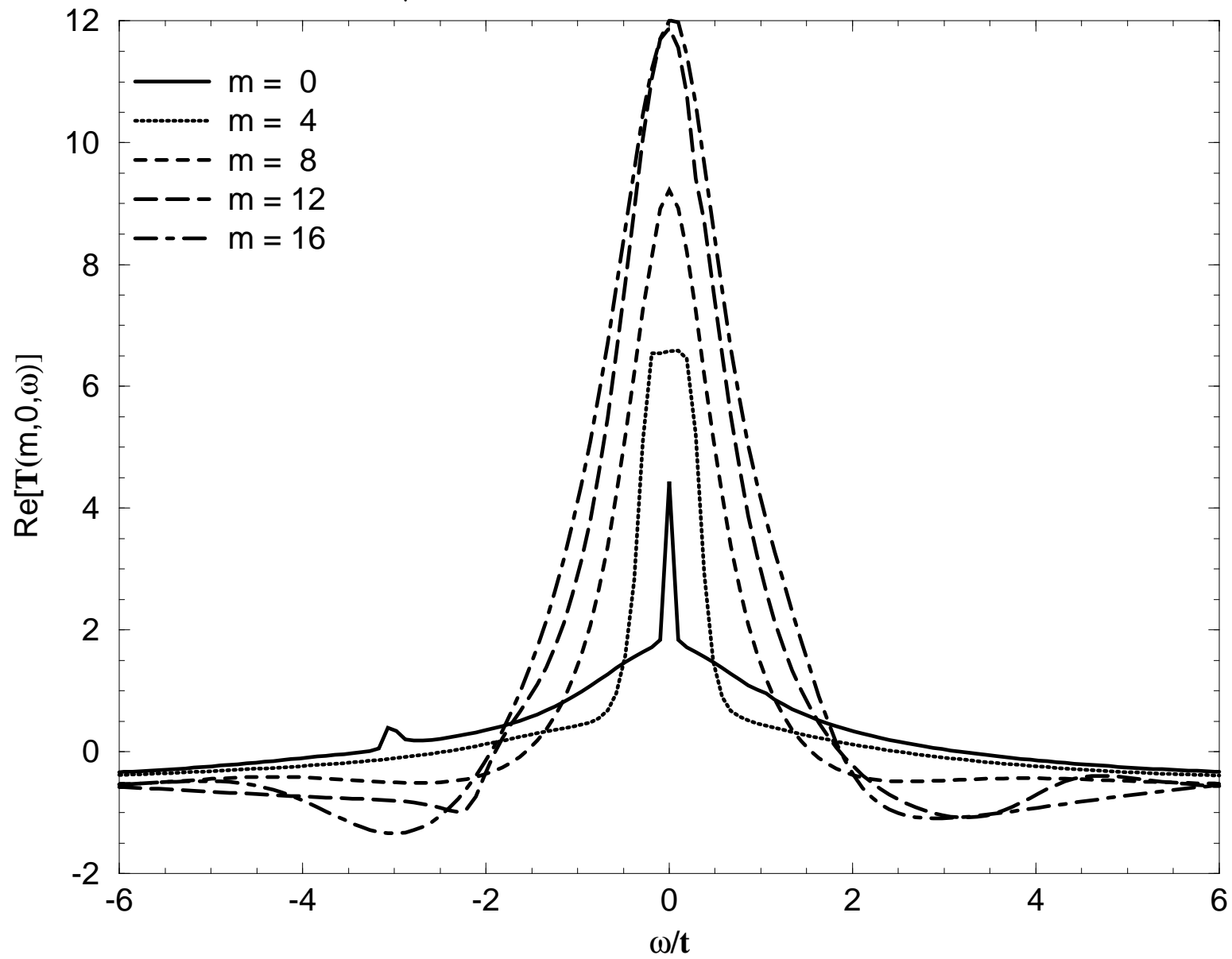
**$U/t = 4.0$   $T/t = 0.03$   $\rho = 0.40$**

**$\mu/t = -0.9558$   $\delta/t = 0.01$   $32*32*1024$**



**$U/t = 4.0$   $T/t = 0.03$   $\rho = 0.40$**

**$\mu/t = -0.9558$   $\delta/t = 0.01$   $32*32*1024$**



**$U/t = 4.0$   $T/t = 0.03$   $\rho = 0.1$**

$\mu/t = -3.17$   $\delta/t = 0.0001$   $32*32*1024$  Flex

